Magnetic Resonance Imaging Parameters in Predicting the Treatment Outcome of High-intensity Focused Ultrasound Ablation of Uterine Fibroids With an Immediate Nonperfused Volume Ratio of at Least 90%

Bilgin Keserci, PhD, Nguyen Minh Duc, MD

Abbreviation

AE
adverse effect

AMH
anti-Mullerian hormone

AUC
area under the curve

DCE
dynamic contrast enhanced

FOV
field of view

GEE
generalized estimating equation

HIFU
high-intensity focused ultrasound

MRI
magnetic resonance imaging

NPV
nonperfused volume

Rationale and Objectives: We aimed to investigate the role of magnetic resonance imaging parameters in predicting the treatment outcome of high-intensity focused ultrasound (HIFU) ablation of uterine fibroids with a nonperfused volume (NPV) ratio of at least 90%.

Material and Methods: A total of 120 women who underwent HIFU treatment were divided into groups 1 ($n = 72$) and 2 ($n = 48$), comprising patients with an NPV ratio of at least 90% and less than 90%, respectively. Multivariate logistic regression analyses were carried out to investigate the potential predictors of the NPV ratio of at least 90%. The NPV ratios immediately post-treatment, therapeutic efficacy at 6 months' follow-up, and safety in terms of adverse effects and changes in anti-Mullerian hormone level were assessed.

Results: By introducing multiple predictors obtained from multivariate analyses into a generalized estimating equation model, the results showed that the thickness of the subcutaneous fat layer in the anterior abdominal wall, peak enhancement of fibroid, time to peak of fibroid, and the ratio of area under the curve of fibroid to myometrium were statistically significant, except T2 signal intensity ratio of fibroid to myometrium, hence predicting an NPV ratio of at least 90%. No serious adverse effects and no significant difference between the anti-Mullerian hormone levels before or 6 months post-treatment were reported.

Conclusions: The findings in this study suggest that the achievement of NPV ratio of at least 90% in magnetic resonance imaging-guided HIFU treatment of uterine fibroids based on prediction model appears clinically possible without compromising the safety of patients.

Key Words: High-intensity focused ultrasound; prediction model; magnetic resonance imaging; therapeutic outcome; uterine fibroids.

Acad Radiol 2018; 25:1257–1269

From the Department of Radiology, Pham Ngoc Thach University of Medicine, 86/2 Thanh Thai, Ward 12, District 10, Ho Chi Minh city, Viet Nam. Received November 29, 2017; revised January 13, 2018; accepted January 18, 2018. **Address correspondence to:** B.K. e-mail: keserci_bilgin@yahoo.com

https://doi.org/10.1016/j.acra.2018.01.022

ROC
receiver operating characteristic

SI
signal intensity

tSSS
transformed symptom severity score

TE
echo time

TR
repetition time

INTRODUCTION

Uterine fibroids, also known as leiomyomas, represent the most common tumor in women. These fibroids disrupt the functions of the uterus and cause menorrhagia, dysmenorrhea, anemia, pelvic pressure or pain, urinary incontinence, recurrent pregnancy loss, and infertility. The lifetime prevalence of uterine fibroids ranges from 70% to 80% (1).

Magnetic resonance imaging (MRI)-guided high-intensity focused ultrasound (HIFU), which combines the anatomical and functional imaging of magnetic resonance (MR) with the thermal ablation possibilities of HIFU, is a promising minimally invasive therapy for the treatment of uterine fibroids. MRI is of great importance in HIFU treatments and not only contributes in patient selection, an essential step toward obtaining good treatment results, but also facilitates planning the treatment, monitoring the safety of the delivery, and verifying the outcome.

Several clinical studies (2–22) have been conducted on T2-weighted (T2W) signal intensity (SI) of uterine fibroids and perfusion MR parameters to determine the extent to which MRI-guided HIFU treatment of uterine fibroids can be performed. The prediction of immediate nonperfused volume (NPV) ratio of more than 60% in earlier studies and 80% in recent studies of HIFU-treated fibroids has been set as a measure of technical success (10,16,17,22).

The immediate NPV ratio, one of the key parameters for determining the therapeutic efficacy, has been on an upward trend to reach almost 100% of the fibroid tumor volume without compromising safety, since the Food and Drug Administration (FDA) relaxed the MRI-guided HIFU treatment guidelines in 2009 (16). Knowledge of T1-weighted (T1W) perfusion and T2W MRI-based parameters before the HIFU treatment might help optimize patient selection and prediction of treatment outcome.

Because patient selection is a significant factor in achieving high NPV ratios, we, in this study, aimed to investigate the role of MRI parameters in predicting the treatment outcome of HIFU ablation with an immediate NPV ratio of at least 90%. In addition, therapeutic efficacy such as fibroid volume reduction and the symptom severity score improvement at 6 months' follow-up, as well as safety in terms of adverse effects (AEs) associated with this strategy and changes in anti-Mullerian hormone (AMH) level were also assessed.

MATERIALS AND METHODS

The study protocol was designed as a retrospective study. The institutional review board approved this study on May 22, 2015. An informed written consent was obtained from each patient before initiation of HIFU-related procedures.

Patients

We considered MRI-guided HIFU treatment for premenopausal women who were 18 years or older, diagnosed with symptomatic uterine fibroids, and agreed to have MRI examinations before and after HIFU treatment. Women participants with endometrial disease or pelvic endometriosis or other uncontrolled systemic disease or positive pregnancy test results or those with intolerance to MRI contrast agents or those with suspected malignancy were excluded from the study.

In our study, 262 women were screened for MRI-guided HIFU treatment. Of these, 120 women (39.5 ± 5.8 years with a range of 22–53 years) with 339 symptomatic uterine fibroids (2.82 per patient, ±3.99 with a range of 1–30), who underwent HIFU treatment between June 2015 and January 2017, were divided into two basic groups: "group 1" comprised patients with an NPV ratio of at least 90% and "group 2" comprised patients with an NPV ratio of less than 90%. Patients in group 2 were further subdivided into three groups in which "subgroup 2A" consisted of patients with an NPV ratio of less than 60%, "subgroup 2B" consisted of patients with an NPV ratio of at least 60% and less than 80%, and "subgroup 2C" consisted of patients with an NPV ratio of at least 80% and less than 90%.

MRI Sequences

All therapies were conducted using a clinical HIFU system (Profound Medical Inc., Toronto, Canada) integrated with a 1.5T MR scanner (Ingenia, Philips, The Netherlands).

First, dynamic contrast-enhanced (DCE) perfusion MRI was carried out during the screening examination as a routine clinical protocol after initiating the intravenous administration of Gd-DO3A-butrol (0.1 mmol/kg of body weight, Gadovist, Bayer Schering Pharma, Germany). The following parameters were used in DCE perfusion MRI: repetition time (TR)/echo time (TE), 4.0/2.0 ms; flip angle (FA), 8°; slice thickness (ST), 5 mm; matrix, 230 × 230; field of view (FOV), 116 × 114 mm; acquisition time, 132 seconds; 50 dynamics (five precontrast and subsequent 45 postcontrast were obtained every 3.6 seconds); and axial plane.

Second, T2W 3D turbo spin echo images were acquired for screening, treatment planning, and 6-month follow-up using the following parameters: TR/TE, 1300/130 ms; FA, 90°; ST, 1.25 mm; matrix, 224 × 218; FOV, 250 × 250 mm; number of slices, 160; acquisition time, 190 seconds; sagittal plane; and sensitivity encoding 2.

Third, multiplane MR thermometry using volumetric techniques (23) was performed using 2D radiofrequency spoiled gradient-recalled echo-planar imaging with the following parameters: TR/TE, 37/19.5 ms; FA, 19°; ST, 7 mm; matrix, 160 × 100; FOV, 400 × 250 mm; acquisition time, 2.9 seconds; echo-planar imaging factor, 11; principle of selective excitation technique fat suppression; and 121-binomial water-selective excitation.

Fourth, a contrast-enhanced (CE) T1W sequence for the evaluation of uterine fibroid characteristics was acquired immediately after HIFU treatment and at 6 months' follow-up based on the following parameters: TR/TE, 5.5/2.7; FA, 10°; IR delay, 90 ms; ST, 1.5 mm; matrix, 150 × 150; FOV, 250 × 250 mm; number of slices, 90; acquisition time, 173 seconds; coronal plane; short tau inversion recovery fat suppression; and sensitivity encoding 1.5.

Assessment of T2W Images and Perfusion MRI

The following parameters were assessed on the basis of T2W images: (1) *baseline parameters* such as diameter of uterine fibroid, uterus position (anteverted or retroverted), fibroid types (intramural, submucosal, or subserosal), distance from the posterior surface of the fibroid to the skin and thickness of the subcutaneous fat layer in the anterior abdominal wall, and (2) *T2 SI parameters* such as SI of uterine fibroids, SI ratio of fibroid to muscle, and SI ratio of fibroid to myometrium.

As described in a previous study (22), in accordance with the enhancement of DCE-MRI during screening, the time-SI curves of fibroid and myometrium were generated and the following *semiquantitative perfusion MR parameters* were calculated: relative enhancement (in percentage), peak enhancement, relative peak enhancement (in percentage), time to peak (in seconds), wash-in rate (per second), washout rate (per second), and area under the curve (AUC). To quantify the time-SI curves on MR T1W perfusion imaging, the ratio of each semiquantitative perfusion parameters was defined as the ratio of the SI of uterine fibroid to the SI of myometrium. The value of washout rate from myometrium was regarded as zero when the SI of the myometrium gradually increased until the end of dynamic imaging (21). This clearly influenced the results of the ratio of perfusion parameters and was therefore not considered in our analysis.

The regions of interest (ROIs) were drawn (1) over the center of the fibroid as large as possible without overlapping with the capsule of fibroid (a region where vessels supply blood to the fibroids), (2) over the myometrium including the maximum area of the smooth muscle tissues while avoiding the surrounding structures, including fibroid and endometrium from both the screening T2W and perfusion MR images; and (3) over the rectus abdominis muscle which includes the maximum area of the skeletal muscle tissues without inclusion of the surrounding structures, only on the T2W MR image.

MR-guided High-intensity Focused Ultrasound Treatment

The therapeutic ultrasound energy was produced by a transducer with a 140-mm focal length that was operated at a frequency of 1.2 or 1.45 MHz and equipped with a mechanical displacement device with five degrees of freedom (three translational and two rotational). The therapy sonication power level (70–300 W) was determined on the basis of the results of an initial test sonication with low power (30–60 W) and adjusted in an iterative manner according to the results of the previous sonications. The treatment cell was ellipsoidal in shape, with a choice of 4, 8, 12, 14, or 16 mm for the axial dimension and 10, 20, 30, 35, or 40 mm for the longitudinal dimension.

Our goal of treatment planning within the permitted timeframe was to target a fibroid volume that was as close to 100% as possible, without sacrificing patient safety. The treatment cells were placed on the T2W planning images, with careful consideration of safety margins from the borders of the treatment cells to critical organs such as the small bowel or sacral bone (1 and 4 cm, respectively). When necessary, urinary bladder filling with normal saline solution or rectal filling with ultrasound gel was performed to displace small bowel loops or move the path of the sonication beam out of the pubic bone area.

Therapeutic Efficacy and Safety Assessment

The immediate NPV ratio was calculated by dividing the post-treatment NPV with the pretreatment fibroid volume. The percentage fibroid volume reduction at 6 months post-treatment was calculated as a proportion of the baseline fibroid volume. The symptom severity score index was evaluated using a questionnaire described by Spies et al. (24). The questionnaire included eight questions on symptom severity. Transformed symptom severity score (tSSS) at screening and at 6 months' follow-up were calculated on a 100-point scale, with higher scores indicating worse symptoms.

Any complications and AEs during HIFU treatment and follow-up period were recorded and graded according to the Society of Interventional Radiology guidelines (25). Furthermore, ovarian reserve was estimated by measuring serum AMH level (26). Blood samples were obtained for the measurement of serum AMH before and 6 months after HIFU treatment. All AMH levels reported in this study were measured in a single run via enzyme-linked immune analysis with an AMH Gen II enzyme-linked immunosorbent assay kit (Beckman Coulter Inc., Brea, CA).

Data Analysis and Statistics

Statistical analysis was performed using SPSS software (version 24.0, 64-bit edition, IBM Corp., Armonk, NY). A 2-sided *P* value less than 0.05 ($P < .05$) was defined the level of significance.

Continuous variables were expressed as mean values ± standard deviation and range. Comparisons of baseline features, fibroid and HIFU procedure characteristics, and therapeutic responses of both groups 1 and 2 were performed using the appropriate statistical test (chi-square test, Fisher exact tests, Mann-Whitney *U* test).

Multivariate logistic regression analyses were carried out in (1) baseline parameter group, (2) T2 SI group, and (3) semiquantitative perfusion group to investigate the potential predictors of the NPV ratio of at least 90% in each group. Using all the significant screening MRI parameters acquired from the multivariate analyses, generalized estimating equation (GEE) was used to predict the treatment outcome of HIFU ablation with an immediate NPV ratio of at least 90%. Cutoff values, AUC, sensitivity, and specificity for the prediction of achieving the treatment intent (ie, NPV ratio of at least 90%) were determined based on receiver operating characteristic (ROC) curve analysis.

RESULTS

Baseline Characteristics

Among the baseline characteristics, subcutaneous fat thickness on abdominal wall was larger in group 2 ($P = .004$). No significant difference was observed between the two groups for any other variables. Table 1 summarizes the baseline features of the study population. There was no instance involving cancellation of HIFU treatment because of technical failure.

Characteristics of MRI-guided HIFU Treatment of Uterine Fibroids

The mean values of acoustic sonication power in groups 1 and 2 were 141.8 ± 21.9 W (90–180 W) and 189.4 ± 43.5 W (110–260 W; $P < .001$), and the corresponding mean treatment durations measured from the first sonication to the last sonication were 148.4 ± 78.4 minutes (41.0–466.0 minutes) and 130.3 ± 42.0 minutes (44.0–239.0 minutes; $P = .146$), respectively. The mean treatment speeds were 1.4 ± 0.7 mL/min (0.13–3.31 mL/min) and 0.6 ± 0.4 mL/min (0.02–1.46 mL/min) in groups 1 and 2, respectively ($P < .001$).

In total, 51 (42.5%) in group 1 and 18 (10.8%) in group 2 required urinary bladder filling (with saline) or rectal filling (with ultrasound gel), whereas 51 patients (42.5%) did not require bowel mitigation. An oral sedative agent (diazepam 5 mg) was administered to patients 30 minutes before treatment. Intravenous drip infusions of an analgesic, paracetamol (1000 mg), and fentanyl citrate (100 μg in 500 mL of normal

TABLE 1. Comparison of Baseline Characteristics According to the NPV Ratio of at Least 90% and Less Than 90%

Characteristics	All Patients	NPV Ratio ≥90%	NPV Ratio <90%	*P* Value
Patients	120	72	48	
Subcutaneous fat thickness (mm)	11.9 ± 4.3 (3.0–26.0)	11.0 ± 4.4 (3.0–25.0)	13.3 ± 3.8 (5.0–26.0)	.004‡
Presence of abdominal scars				
Yes	31	17	14	.528
No	89	55	34	
Uterus position				.060
Anteverted	87	48	39	
Retroverted	33	24	9	
Diameter (cm)*	7.1 ± 2.6 (2.4–15.1)	7.3 ± 3.0 (2.4–15.1)	6.8 ± 1.9 (3.0–11.8)	.337
Distance (mm)†	94.5 ± 15.0 (57.0–133.0)	94.1 ± 15.6 (57.0–130.0)	95.2 ± 14.2 (59.0–133.0)	.686
Fibroid types				.526
Intramural	68	38	30	
Subserosal	21	13	8	
Submucosal	31	21	10	

NPV, nonperfused volume.

Values in parentheses represent ranges.

* Largest treated fibroids only.

† From skin to the most posterior part of the largest fibroid.

‡ Statistically significant.

saline) were routinely administered before initiating the treatment.

Although all 339 fibroids were treated, only the largest fibroid (ie, the most symptomatic one) per patient was considered for analysis in this study. Of the 120 fibroids, the mean diameter in groups 1 and 2 were 7.3 ± 3.0 cm (2.4–15.1 cm) and 6.8 ± 1.9 cm (3.0–11.8 cm), respectively. There were 72 patients who had NPV ratio of at least 90% and the remaining 48 patients had an NPV ratio of less than 90%. The mean NPV ratio for group 1 (patients with NPV ratio of at least 90%) was 97.7% ± 3.2 (90–100%) and group 2 (patients with an NPV ratio of less than 90%) was 60.4% ± 27.3 (4.2–89.8%). In group 1, the NPV ratio was 100% in 41 patients and at least 90% but less than 100% in 31 patients. In group 2, NPV ratio was less than 60% (subgroup 2A) in 17 patients, at least 60% but less than 80% (subgroup 2B) in 17 patients, and at least 80% and less than 90% (subgroup 2C) in 14 patients. Figures 1a-c and 2a-c show an example of pre-HIFU perfusion MRI data, pre-HIFU T2W MR images, and immediate post-HIFU CE-T1W MR images according to the NPV ratio of at least 90% and less than 90%, respectively.

Analysis of Factors Influencing NPV Ratio of at Least 90%

In multivariate analyses using an enter method, an NPV ratio of at least 90% was set as dependent variable, whereas the factors in each group (ie, baseline, T2 SI, and semiquantitative perfusion MR parameters) that possibly affect the treatment outcome were set as independent variables.

The results of multivariate analyses revealed that there were five statistically significant predictors ($P < .05$): thickness of the subcutaneous fat layer in the anterior abdominal wall, SI ratio of fibroid to myometrium, peak enhancement of fibroid, time to peak of fibroid, and the ratio of AUC of fibroid to myometrium (Table 2).

Prediction Model

The GEE analysis produced the model

$$\gamma = \frac{e^{-6.958+0.143\times1+0.189\times2+0.008\times3-0.015\times4+4.785\times5}}{1+e^{-6.958+0.143\times1+0.189\times2+0.008\times3-0.015\times4+4.785\times5}}$$

for predicting an NPV ratio of at least 90% with five statistically significant predictors from multivariate analyses, where ×1 = thickness of the subcutaneous fat layer in the anterior abdominal wall (millimeters), ×2 = T2 SI ratio of fibroid to myometrium, ×3 = peak enhancement of fibroid, ×4 = time to peak of fibroid (in seconds), and ×5 = ratio of AUC of fibroid to myometrium. All the perfusion MRI parameters (ie, ×3, ×4, and ×5) and baseline parameter (ie, ×1) were statistically significant ($P < .05$, Table 3), with the exception of T2 SI ratio of fibroid to myometrium (ie, ×2; $P = .715$, Table 3).

The ROC analysis revealed that the cutoff value for predicting the achievement of treatment intent in terms of NPV ratio of at least 90% was 0.071 (AUC, 0.948; sensitivity, 0.958, specificity, 0.875) (Fig 3).

Assessment of 6 Months' Follow-Up: Fibroid Volume and Symptom Changes

The 6-month fibroid volume reduction ratios in groups 1 and 2 were 0.54 ± 0.13 (0.3–0.84; $n = 72$) and 0.14 ± 0.21 (–0.21 to 0.70; $n = 48$), respectively. In addition, the volume reduction ratio was –0.05 ± 0.11 (–0.21 to 0.2; $n = 17$) in subgroup 2A, 0.07 ± 0.08 (–0.1 to 0.2; $n = 17$) in subgroup 2B, and 0.38 ± 0.19 (0.07–0.7; $n = 14$) in subgroup 2C.

The tSSS in groups 1 ($n = 72$) and 2 ($n = 48$) had decreased from 56.1 ± 16.6 (21.9–87.5) and 60.4 ± 14.9 (31.3–93.8) at baseline to 8.0 ± 9.1 (0.0–43.8) and 46.9 ± 26.5 (0.0–100.0) at 6 months post-treatment, corresponding to improvement ratios of 0.86 ± 0.14 (0.5–1.0) and 0.26 ± 0.37 (–0.25 to 1.0), respectively. In addition, mean tSSS improvement ratio was –0.01 ± 0.15 (–0.25 to 0.21; $n = 17$) in subgroup 2A, 0.18 ± 0.25 (–0.06–0.89; $n = 17$) in subgroup 2B, and 0.67 ± 0.3 (0.11–1.0; $n = 14$) in subgroup 2C.

The fibroid volume reduction and symptom improvement were found to be better in patients with higher NPV ratio (Fig 4, Table 4).

Safety Assessments

AEs in groups 1 and 2 included the following: (1) first-degree skin burn that was resolved without intervention within 12 hours; (2) second-degree skin burn that received conservative treatment and resolved within 7 days upon treatment with antibiotics and anti-inflammatory drugs (1 g amoxicillin-clavulanic acid and 500 mg paracetamol; two times per day); (3) pain manifested as mild pain in the pelvic area, back, and leg during and after HIFU treatment that was treated by an oral analgesic agent (ibuprofen, 400 mg; three times per day) and resolved within 3–7 days in all cases; (4) appearance of abnormal vaginal discharge that disappeared after 14–21 days; (5) Foley catheterization-related cystitis symptoms that subsided with the help of antibiotics amoxicillin-clavulanic acid 1 g; two times per day in 7 days; (6) numbness of the leg that spontaneously resolved after 14–30 days; and (7) self-limiting nausea lasting for less than 1 hour. All these AEs were considered Society of Interventional Radiology class A (no medical intervention required). There was no significant difference in the incidence of each type of complication between the two groups ($P > .05$). Table 5 presents each type of complications according to an NPV ratio of at least 90% and less than 90%.

The AMH levels before and at 6 months post-treatments were 1.98 ± 1.86 (0.03–9.23) and 1.97 ± 1.85 (0.02–9.2; $P = .077$; $n = 72$) in group 1 and 1.81 ± 1.42 (0.21–7.1) and 1.79 ± 1.42 (0.21–7.1; $P = .06$; $n = 48$) in group 2, respectively. In addition, the AMH levels before and 6 months post-treatments were 2.59 ± 1.8 (0.53–7.1) and 2.55 ± 1.83 (0.53–7.1; $P = .119$; $n = 17$) in subgroup 2A, 1.0 ± 0.74 (0.21–2.96) and 1.0 ± 0.73 (0.21–2.96; $P = .083$; $n = 17$) in subgroup 2B,

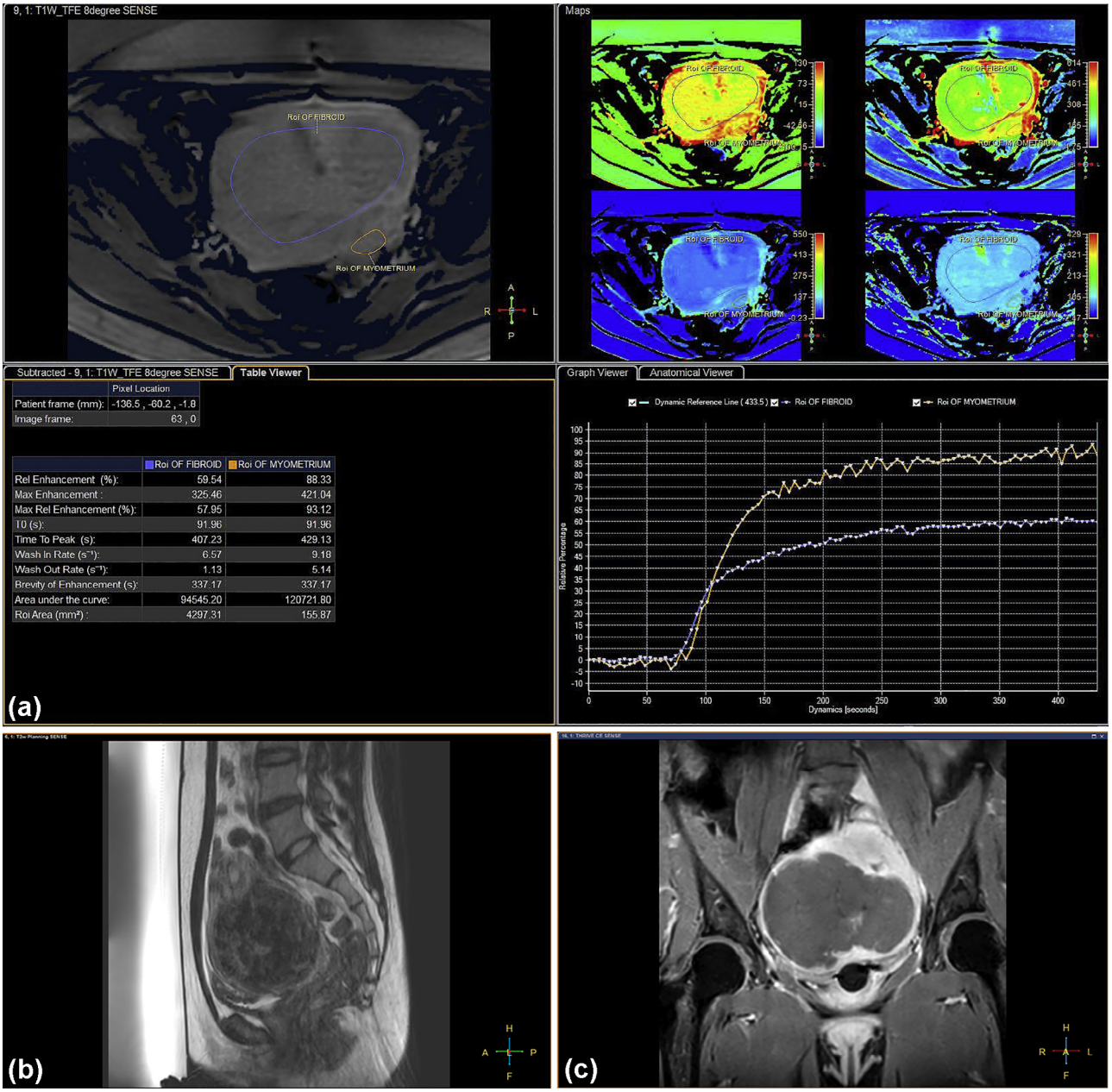

Figure 1. A 33-year-old woman with 11.6-cm uterine fibroid was treated with MRI-guided HIFU ablation. Before HIFU ablation, this patient was classified into Funaki type II and Group A based on T2W SI (5) of uterine fibroids and perfusion MR (22) parameters, respectively. **(a)** A semiquantitative perfusion MR image was analyzed by drawing an ROI within the area of the fibroid and the myometrium on one of the perfusion MR images (upper left, left section). The software automatically calculated the semiquantitative perfusion parameters (lower left, left section) and generated maps of each perfusion parameter (upper right, right section). The time-intensity curve of the fibroid is lower than that of the myometrium (lower right, right section). **(b)** A sagittal T2W MR images of uterine fibroids at screening. **(c)** A contrast-enhanced T1-weighted MR image obtained immediately after MRI-guided HIFU treatment from the NPV ratio of 100% (ie, group 1 which comprised patients with an NPV ratio of at least 90%). HIFU, high-intensity focused ultrasound; MR, magnetic resonance; MRI, magnetic resonance imaging; NPV, nonperfused volume; ROI, region of interest; SI, signal intensity; T2W, T2-weighted.

and 1.84 ± 0.96 (0.88–4.15) and 1.83 ± 0.97 (0.88–4.14; $P = .261$; $n = 14$) in subgroup 2C, respectively. There was no significant difference between the AMH levels before or 6 months post-treatment. None of the patient became amenorrheic or reported symptoms suggestive of menopause. The comparison of AMH levels for the NPV ratio of at least 90% and less than 90% are shown in Figure 5.

DISCUSSION

MRI-guided HIFU treatment of uterine fibroids is being increasingly used worldwide because of its excellent therapeutic efficacy in providing symptomatic relief. Despite the clinical efficacy of this approach, as shown in previous studies (5,9,17,19–21), it is less effective or infeasible in conditions

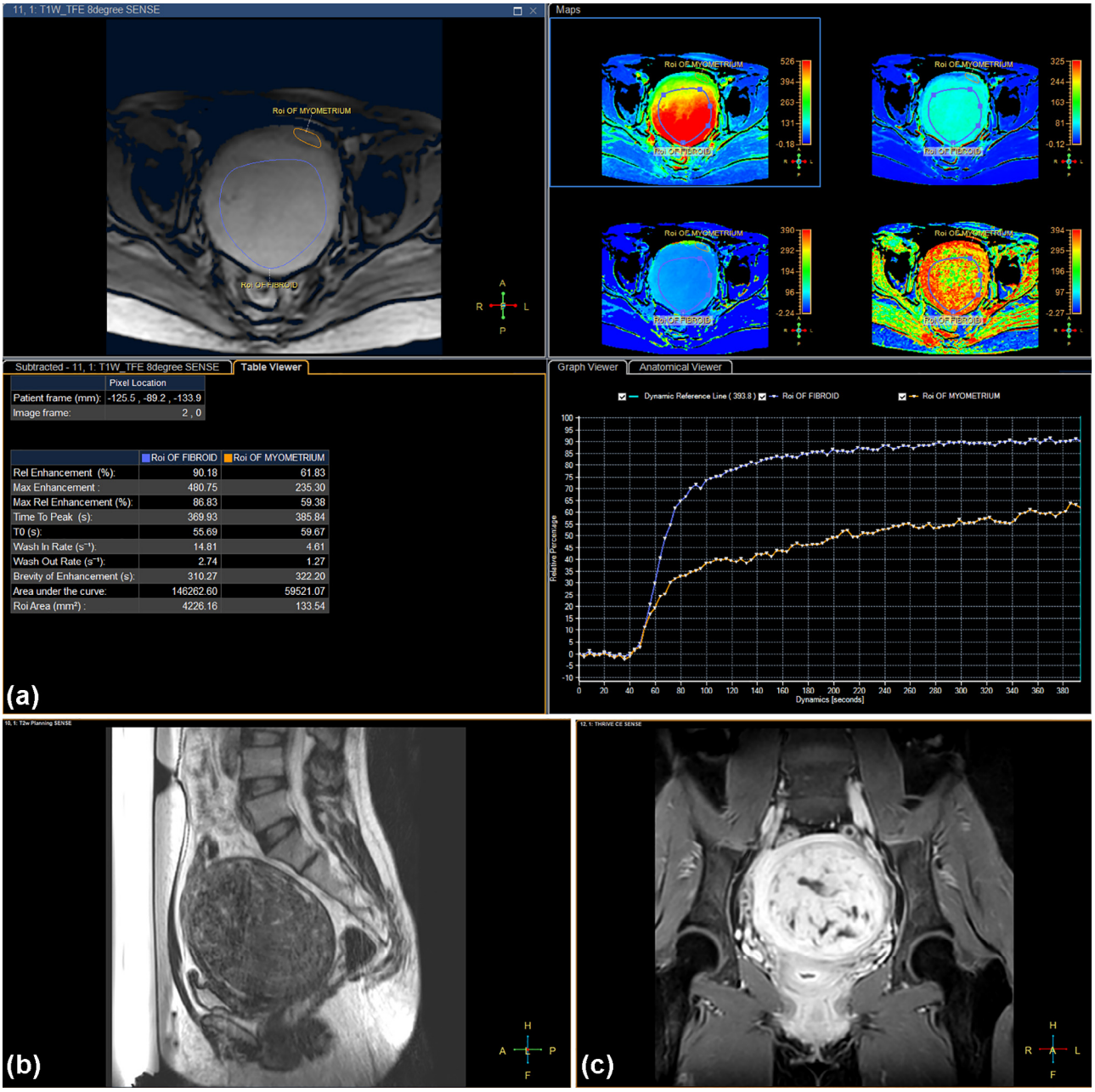

Figure 2. A 34-year-old woman with 12.0-cm uterine fibroid was treated with MRI-guided HIFU ablation. Before HIFU ablation, this patient was classified into Funaki type II and Group B based on T2W SI (5) of uterine fibroids and perfusion MR (22) parameters, respectively. **(a)** A semiquantitative perfusion MR image was analyzed by drawing an ROI within the area of the fibroid and the myometrium on one of the perfusion MR images (upper left, left section). The software automatically calculated the semiquantitative perfusion parameters (lower left, left section) and generated maps of each perfusion parameter (upper right, right section). The time-intensity curve of the fibroid is lower than that of the myometrium (lower right, right section). **(b)** A sagittal T2W MR images of uterine fibroids at screening. **(c)** A contrast-enhanced T1W MR images obtained immediately after MRI-guided HIFU treatment from the NPV ratio of 10% (ie, group 2 which comprised patients with an NPV ratio of less than 90%). HIFU, high-intensity focused ultrasound; MR, magnetic resonance; MRI, magnetic resonance imaging; NPV, nonperfused volume; ROI, region of interest; SI, signal intensity; T1W, T1-weighted; T2W, T2-weighted.

attributed to different tissue properties, such as high SI on T2W MRI and high vascularity on perfusion MRI that are known to be resistive to HIFU heating and are difficult to overcome. Therefore, the role of each MRI parameter in screening phase must be considered to predict the treatment outcome of HIFU ablation. To the best of our knowledge, the present work is the first of its kind that introduces a GEE model for predicting an NPV ratio of at least 90% with statistically significant predictors obtained from multivariate analyses based on MRI parameters.

By introducing multiple predictors (Table 2) into a GEE model, the results of our study showed that the thickness of

TABLE 2. Independent Factors of Each Group Associated With an NPV Ratio of at Least 90%: Multivariate Analysis

Parameters	Multivariate Analysis		
	Estimate	95% CI	*P* Value
Baseline parameters			
Intercept	−3.025	−6.176 to 0.126	.060
Uterus position	0.879	−0.198 to 1.955	.110
Subcutaneous fat thickness (mm)	0.117	0.018–0.215	.021*
Fibroid diameter (cm)	−0.012	−0.030 to 0.006	.188
Distance (mm)*	0.013	−0.017 to 0.043	.403
Fibroid type	0.480	−0.698 to 1.657	.424
T2 SI parameters			
Intercept	−1.978	−3.051 to −0.906	<.001
SI of uterine fibroids	0.004	−0.003 to 0.010	.257
SI ratio of fibroid to muscle	0.187	−0.150 to 0.525	.277
SI ratio of fibroid to myometrium	1.236	0.045–2.427	.042†
Semiquantitative perfusion MR parameters			
Intercept	−6.055	−11.671 to −0.439	.035
Relative enhancement (in percentage)	−0.001	−0.063 to 0.061	.971
Peak enhancement	0.006	0.00005 to 0.012	.048†
Relative peak enhancement (in percentage)	−0.007	−0.071 to 0.058	.832
Time to peak (in seconds)	−0.009	−0.017 to −0.001	.021†
Wash-in rate (per second)	0.093	−0.011 to 0.196	.079
Area under the curve	−0.00001	−0.00003 to 0.000006	.220
Ratio of relative enhancement of fibroid to myometrium	−1.099	−5.590 to 3.392	.632
Ratio of peak enhancement of fibroid to myometrium	−3.096	−6.313 to 0.120	.059
Ratio of relative peak enhancement of fibroid to myometrium	3.108	−1.398 to 7.615	.176
Ratio of time to peak of fibroid to myometrium	0.381	−1.740 to 2.501	.725
Ratio of wash-in rate of fibroid to myometrium	−0.261	−1.829 to 1.308	.745
Ratio of area under the curve of fibroid to myometrium	6.307	1.337–11.277	.013†

CI, confidence interval; MR, magnetic resonance; NPV, nonperfused volume; SI signal intensity.

* From skin to the most posterior part of the largest fibroid.

† Statistically significant.

TABLE 3. Results of Generalized Estimating Equation (GEE) Analyses for Predicting the Treatment Outcome of MRI-guided HIFU Ablation With an NPV Ratio of at Least 90%

Parameters	Estimate	Standard Error	95% CI	*P* Value
Intercept	−6.958	2.385	−11.633 to −2.282	.004
Subcutaneous fat thickness (mm)	0.143	0.065	0.014–0.271	.030*
SI ratio of fibroid to myometrium	0.189	0.518	−0.826 to 1.205	.715
Peak enhancement	0.008	0.002	0.003–0.012	.001*
Time to peak (in seconds)	−0.015	0.004	−0.023 to −0.007	.001*
Ratio of area under the curve of fibroid to myometrium	4.785	1.666	1.519–8.051	.004*

CI, confidence interval; HIFU, high-intensity focused ultrasound; MRI, magnetic resonance imaging; NPV, nonperfused volume; SI, signal intensity.

* Statistically significant.

the subcutaneous fat layer in the anterior abdominal wall, peak enhancement of fibroid, time to peak of fibroid, and the ratio of AUC of fibroid to myometrium were statistically significant, except T2 SI ratio of fibroid to myometrium, hence predicting an NPV ratio of at least 90% (Table 3).

During HIFU treatment, the ultrasound beam penetrates through the cutaneous, subcutaneous, and other intermediate tissue layers before reaching the focus in the fibroid. Because all biological tissues absorb ultrasound energy to various extents, the increase in deposited energy might inevitably lead to a temperature rise in the near-field of the ultrasound beam path between the transducer and the focal point. Temperature rise within the skin occurs mainly in the subcutaneous tissue due to its lower specific heat capacity (27), insulator properties (28,29), and lower blood supply (30) than that of other tissues in the abdominal wall. In another study (11), the thickness

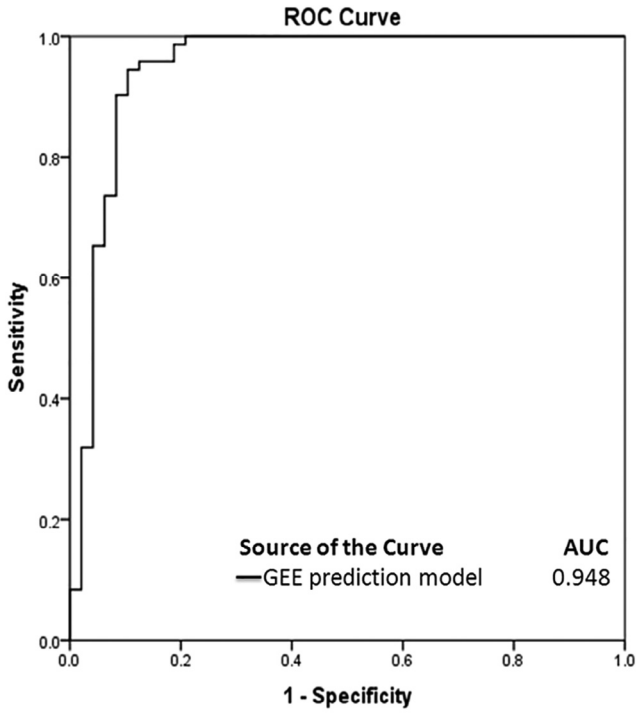

Figure 3. The ROC curves of the prediction model in predicting the treatment outcome of HIFU ablation with an immediate NPV ratio of at least 90%. AUC, sensitivity, and specificity were 0.948, 0.958, and 0.875, respectively. AUC, area under the curve; HIFU, high-intensity focused ultrasound; NPV, nonperfused volume; ROC, receiver operating characteristic.

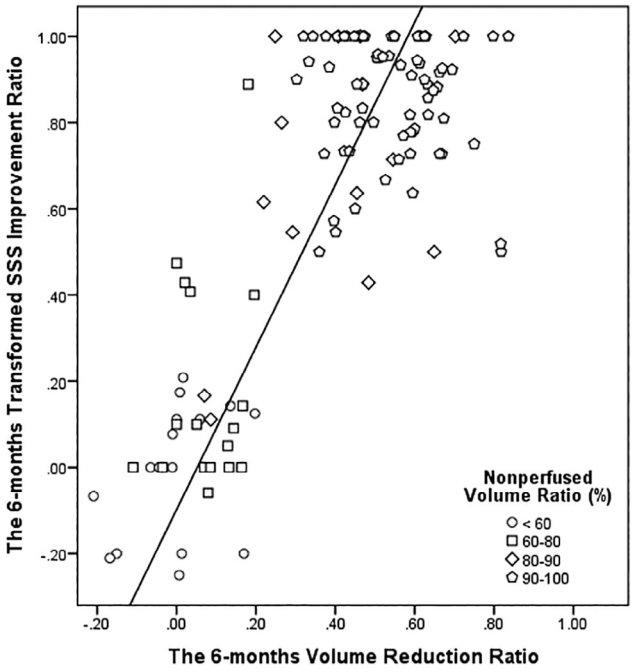

Figure 4. The scatter plot of tSSS improvement ratios against fibroid volume reduction ratios at 6 months for each patient among different groups as a function of NPV ratios (ie, <60%, ≥60% and <80%, ≥80% and <90%, and ≥90%). NPV, nonperfused volume; tSSS, transformed symptom severe score.

of the subcutaneous and ventral visceral fat tissue of the target uterine fibroid was larger than 20 mm (in diameter). Mikami et al. (11) suggested that thick subcutaneous or visceral fat tissue attenuated the sonication's exposure energy and caused insufficient elevation in temperature at the target area. In a recent study (19), the subcutaneous fat thickness proved to be a significant influence on the HIFU ablation of uterine fibroids. In our study, multivariate analysis of baseline parameters also suggested that the thickness of the subcutaneous fat layer in the anterior abdominal wall ($P = .021$) might be a valuable predictor of the outcome of HIFU ablation with an NPV ratio of at least 90%; these findings concur with results of previous studies (11,17).

Uterine fibroids with different SIs on T2W MRI have different biological characteristics (31) resulting in different HIFU ablation effects (9,12,32). The Funaki classification (6) comparing the mean T2W SI of the fibroid to that of the skeletal muscle and myometrium is used as the primary MRI classification parameter for determining patient suitability, by dividing the patient population in three groups (types I, II, and III). A study reported that the uterine fibroids in the failure group demonstrated heterogeneous and high SI relative to the myometrium on T2W MR images, whereas the uterine fibroids in the success group demonstrated low SI relative to the myometrium (11). In a recent study (19), multivariate analysis revealed that high T2 SI ratio of uterine fibroid to skeletal muscle was one of the significant parameters attributing to poor heating efficiency of HIFU ablation. In our study, in addition to SI of uterine fibroid and SI ratio of fibroid to muscle, we also included SI ratio of fibroid to myometrium in the multivariate analysis of T2 SI group, as the uterine fibroids are characterized by the proliferation of smooth muscle cells in the myometrium. Among T2 SI group parameters, SI ratio of fibroid to myometrium was the strongest predictor ($P = .042$), predicting the treatment outcome of HIFU ablation with an NPV ratio of at least 90%. These findings of our study are also in line with previous studies (5,22), which considered myometrium as an internal reference.

Moreover, one case report (33) showed that high T2 SI fibroids that exhibit delayed enhancement in DCE MR images could be treated successfully if the hyperintensity was a result of high fluid content rather than high vascularity. In another study (17), although the NPV ratio of fibroids characterized by low SI in CE T1W images was significantly high, the same could not be effectively predicted by T2 SI. These studies explain that T2 SI of the uterine fibroid could not differentiate high SI between vascularity and water from edematous and degeneration. Furthermore, according to bivariate analysis in our study, the T2 SI ratio of fibroid to myometrium showed positive correlation with the thickness of the subcutaneous fat layer in the anterior abdominal wall ($r = 0.207$, $P = .023$) and the ratio of AUC of fibroid to myometrium ($r = 0.191$, $P = .036$). These might explain why the T2 SI ratio of fibroid to myometrium was not statistically significant in the GEE prediction model. This is in line with Pennes' equation (34) in which the blood perfusion might be a predominant

TABLE 4. Comparison of Fibroid Tumor Volume and Symptom Changes Based on the NPV Ratio of at Least 90% and Less Than 90%

Treatment Outcome	All Patients (n = 120)	NPV Ratio ≥90% (n = 72)	NPV Ratio <90% (n = 48)	P Value
Fibroid volume (mL)*				
Baseline				.011‡
Mean ± SD	197.3 ± 155.7	226.7 ± 181.6	153.2 ± 90.7	
Range	6.0–794.0	6.0–794.0	12.0–478.0	
6 mo				.004‡
Mean ± SD	113.2 ± 89.3	94.4 ± 70.8	141.4 ± 106.1	
Range	4.0–578.0	4.0–400.0	10.0–578.0	
Reduction ratio				.001‡
Mean ± SD	0.38 ± 0.26	0.54 ± 0.13	0.14 ± 0.21	
Range	–0.21–0.84	0.30–0.84	–0.21 to0.70	
Symptom severity score†				
Baseline				.151
Mean ± SD	57.8 ± 16.0	56.1 ± 16.6	60.4 ± 14.9	
Range	21.9–93.8	21.9–87.5	31.2–93.	
6 mo				.001‡
Mean ± SD	23.6 ± 26.3	8.0 ± 9.1	46.9 ± 26.5	
Range	0.0–100.0	0.0–43.8	0.0–100.0	
Improvement ratio				.001‡
Mean ± SD	0.62 ± 0.39	0.86 ± 0.14	0.26 ± 0.37	
Range	–0.25–1.0	0.5–1.0	–0.25 to 1.0	

NPV, nonperfused volume; SD, standard deviation.

* Largest treated fibroid only.

† Transformed symptom severe score (tSSS) can range from 0 to 100.

‡ Statistically significant.

TABLE 5. Complications and Adverse Effects of MRI-guided HIFU Treatment According to the NPV Ratio of at Least 90% and Less Than 90%

SIR Classification	All Patients (n = 120)	NPV Ratio ≥90% (n = 72)	NPV Ratio <90% (n = 48)	P Value
Class A				
Skin burn grade 1	3 (2.5)	0 (0)	3 (6.25)	.062
Skin burn grade 2	1 (0.83)	0 (0)	1 (2.1)	.400
Back pain	8 (6.7)	3 (4.2)	5 (10.4)	.264
Pelvic pain	12 (10)	10 (13.9)	2 (4.2)	.121
Leg pain	12 (10)	8 (11.1)	4 (8.3)	.761
Nausea	6 (5)	6 (8.3)	0 (0)	.080
Numbness	12 (10)	8 (11.1)	4 (8.3)	.761
Vaginal discharge	13 (10.8)	10 (13.9)	3 (6.25)	.154
Cystitis	1 (0.83)	1(1.4)	0 (0)	1.000

HIFU, high intensity focused ultrasound; MRI, magnetic resonance imaging; NPV, nonperfused volume; SIR, Society of Interventional Radiology. Values in parentheses represent percentages.

parameter affecting temperature rise in predicting the HIFU treatment outcomes.

Perfusion MRI is the most robust MR technique for the assessment of uterine fibroid vascularity and can help to assess whether and to what extent the fibroid is perfused. Kim et al. reported that the relative peak enhancement in semiquantitative perfusion MRI were significantly associated with the treatment efficiency of HIFU ablation of uterine fibroid (19). In our study, according to multivariate analysis of semiquantitative perfusion MR parameters, peak enhancement of fibroid (P = .048), time to peak of fibroid (P = .021) and the ratio of AUC of fibroid to myometrium (P = .013) were the significant parameters for predicting the treatment outcome of HIFU ablation with an NPV ratio of at least 90%. Peak enhancement manifests the maximum vascularity of the fibroid, which might explain why it is difficult to achieve heat accumulation in group 2 patients. Another important issue that affects heat accumulation is the blood flow velocity. Blood flow usually drains the delivered heat from the heated region, which in turn causes insufficient thermal dose delivery at the

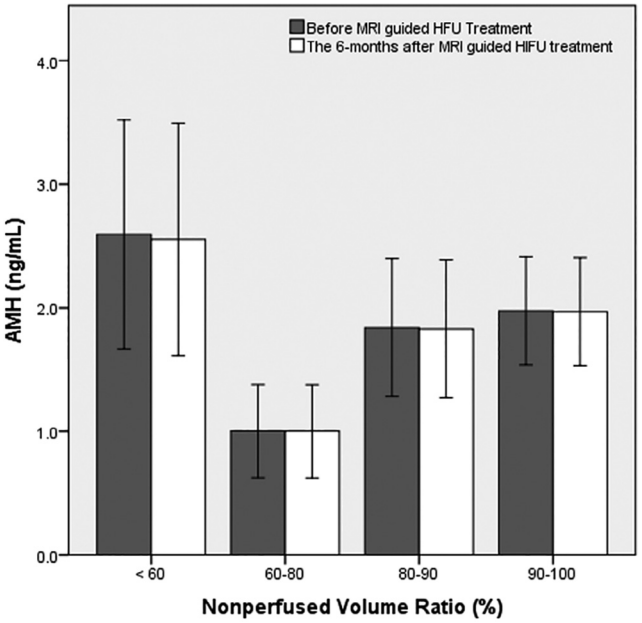

Figure 5. The box plot represents the serum AMH levels before and 6 months after MRI-guided HIFU treatment according to the NPV ratio of at least 90%, less than 90% but at least 80%, less than 80% but at least 60%, and less than 60%. Data are given as box-and-whisker plot. AMH, anti-Mullerian hormone; HIFU, high-intensity focused ultrasound; MRI, magnetic resonance imaging; NPV, nonperfused volume.

targeted volume. This is a factor that needs careful consideration in thermal treatments, and in determining why ablation is more efficient in group 1 patients. Lastly, the ratio of AUC of fibroid tissue to myometrium is another significant parameter for the treatment of MRI-guided HIFU ablation of uterine fibroids. In a previous study (22), a new classification method was introduced based on MR T1 perfusion-based time-SI curves of fibroid tissue compared to myometrium in screening MRI, for predicting the treatment outcome of HIFU ablation with an NPV ratio of at least 80%. As the tissue density of the myometrium is low and the moisture content is high (35), HIFU treatment has minimal effects on the normal myometrium, which can explain the low NPV ratio in treatment outcomes in group 2 patients, especially in subgroups 2A and 2B. Our findings concur with results of previous studies (19,22).

The ROC curve presented here (Fig 3) allows the clinician to estimate the probability of a patient achieving an NPV ratio of at least 90% in MRI-guided HIFU treatment of uterine fibroids. The choice of a cutoff value for predicting NPV ratio of at least 90% is difficult because of the implicit trade-offs between sensitivity and specificity. In other words, the prediction model introduced in this study and cutoff values based on GEE model will either rule out the patients who have lower chance of achieving an NPV ratio of at least 90% (with high sensitivity) or introduce the eligible patients with high confidence of achieving an NPV ratio of at least 90% (with high specificity).

In the present study, the therapeutic efficacy of MRI-guided HIFU treatment was evaluated on the extent of fibroid volume reduction and improvement in tSSS at 6 months post-treatment. Of the 120 follow-up patients, the present study confirmed that the fibroid volume reduction was significantly greater in group 1 compared to group 2 ($P < .001$; Table 4). In addition, in the subgroup analysis of the patients with an NPV ratio of less than 90% ($n = 48$), the fibroid volume reduction was also statistically significant among the three subgroups: (1) the fibroid volume reduction ratio was significantly greater in patients with an NPV ratio of at least 80% and less than 90% ($n = 14$) compared to the patients with an NPV ratio of at least 60% and less than 80% ($n = 17$, $P < .001$); (2) the fibroid volume reduction ratio was significantly greater in patients with an NPV ratio of at least 60% and less than 80% ($n = 17$) compared to the patients with an NPV ratio of less than 60% ($n = 17$, $P < .001$); and (3) the fibroid volume reduction ratio was also significantly greater in patients with an NPV ratio of at least 80% and less than 90% ($n = 14$) compared to the patients with an NPV ratio of less than 60% ($n = 17$, $P < .001$). These concur with one of the earlier studies (13) that reported 31% of volume reduction at 6 months' follow-up and one of the latest studies (16) that reported 43% and 20% of volume reduction at 3 months' follow-up in patients with an NPV ratio of at least 80% and less than 80%, respectively.

The mean tSSS improvement was significantly greater in group 1 compared to group 2 ($P < .001$; Table 4). In group 2, the tSSS improvement was also statistically significant among the three subgroups ($P < .001$). A clinically significant reduction of tSSS by at least 10 points (4,13,15,16), was achieved in 83.3% of the patients. The remaining 16.7% of the patients with less than 10 points improvement were in subgroups 2A ($n = 11$) and 2B ($n = 9$).

The AEs encountered in this study were typically manifested interprocedurally and resolved shortly thereafter. First- and second-degree skin burns were observed in four patients in group 2. These incidents only occurred during the early phase of HIFU treatment, owing to lack of operator experience. As shown in Table 5, most common complaints were (1) back pain due to extended procedure in the prone position; (2) leg pains and numbness due to the location of the fibroid or stimulation of the sciatic nerve by ultrasound sonication energy (4); and (3) pelvic pain and vaginal discharge due to local edema of the treated region or uterus contraction. Additionally, cystitis was attributed to Foley catheterization. The results of the present study demonstrated that the achievement of an NPV ratio of at least 90% could be possible within an acceptably low complication rate without compromising safety. These complications are known AEs of HIFU treatment of uterine fibroids, and the findings are in line with the results of previous clinical studies on MRI-guided HIFU treatments of uterine fibroids (16,17).

With the achievement of an NPV ratio of at least 90% in MRI-guided HIFU treatment of uterine fibroids, it is important to consider the potential impact of the procedures on

the ovarian reserve because ovarian dysfunction can lead to accelerated onset of menopause and diminished fertility. The effect on ovarian reserve of hysterectomy and uterine artery embolization for treating uterine fibroids has been a matter of concern as reported by the measurements of serum AMH levels at baseline and post-treatment (36–38). In this study, despite a relatively small number of patients in each group and a relatively short follow-up period, we found that there was no significant change in AMH levels before and 6 months after HIFU treatment (Fig 5), suggesting that the ovary and its vessels were not involved in the treatment area even for an NPV ratio of at least 90% prediction. Therefore, HIFU ablation did not damage the ovarian blood flow, and this finding is in agreement with recent studies (39,40).

There were some limitations in the present study. First, because of the single-center retrospective study design, further prospective multicenter studies are required for validation of the role of MRI parameters in predicting the treatment outcome of HIFU ablation of uterine fibroids with an NPV ratio of at least 90%. Second, in our study, we only investigated MRI screening parameters for predicting an NPV ratio of at least 90%. Future studies must also include HIFU treatment parameters, including treatment cell size, degree of overlapping treatment cells, ablation with one or multilayer treatment strategy, sufficient cooling time between each sonication, and selection of acoustic power within a given safety limit, for larger scale evaluation of the role of introduced model in predicting the treatment outcome of HIFU ablation of uterine fibroids with an NPV ratio of at least 90%. Third, other markers such as serum follicle-stimulating hormone, serum estradiol, serum progesterone, and ovarian volume were not assessed in this study. Fourth, the follow-up period in this study was 6 months; follow-up over a year or more would be better for evaluation of treatment efficacy and safety.

CONCLUSION

The present retrospective study demonstrated that the achievement of NPV ratio of at least 90% in MRI-guided HIFU treatment of uterine fibroids using multivariate analyses and prediction model as a measure of technical success appears to be clinically possible. Moreover, the preliminary findings in the therapeutic efficacy at 6 months' follow-up showed that HIFU should aim to achieve the maximum possible NPV ratio without compromising the safety of patients.

REFERENCES

1. Baird DD, Dunson DB, Hill MC, et al. High cumulative incidence of uterine leiomyoma in black and white women: ultrasound evidence. Am J Obstet Gynecol 2003; 188:100–107.
2. Tempany CM, Stewart EA, McDannold N, et al. MR imaging-guided focused ultrasound surgery of uterine leiomyomas: a feasibility study. Radiology 2003; 226:897–905.
3. Stewart EA, Gedroyc WM, Tempany CM, et al. Focused ultrasound treatment of uterine fibroid tumors: safety and feasibility of a noninvasive thermoablative technique. Am J Obstet Gynecol 2003; 189:48–54.
4. Hindley J, Gedroyc WM, Regan L, et al. MRI guidance of focused ultrasound therapy of uterine fibroids: early results. AJR Am J Roentgenol 2004; 183:1713–1719.
5. Funaki K, Fukunishi H, Funaki T, et al. Magnetic resonance-guided focused ultrasound surgery for uterine fibroids: relationship between the therapeutic effects and signal intensity of preexisting T2 weighted magnetic resonance images. Am J Obstet Gynecol 2007; 196.
6. Funaki K, Fukunishi H, Funaki T, et al. Mid-term outcome of magnetic resonance-guided focused ultrasound surgery for uterine myomas: from six to twelve months after volume reduction. J Minim Invasive Gynecol 2007; 14:616–621.
7. Stewart EA, Gostout B, Rabinovici J, et al. Sustained relief of leiomyoma symptoms by using focused ultrasound surgery. Obstet Gynecol 2007; 110:279–287.
8. Funaki K, Sawada K, Maeda F, et al. Subjective effect of magnetic resonance-guided focused ultrasound surgery for uterine fibroids. J Obstet Gynaecol Res 2007; 33:834–839.
9. Lenard ZM, McDannold NJ, Fennessy FM, et al. Uterine leiomyomas: MR imaging-guided focused ultrasound surgery—imaging predictors of success. Radiology 2008; 249:187–194.
10. Morita Y, Ito N, Hikida H, et al. Non-invasive magnetic resonance imaging-guided focused ultrasound treatment for uterine fibroids—early experience. Eur J Obstet Gynecol Reprod Biol 2008; 139:199–203.
11. Mikami K, Murakami T, Okada A, et al. Magnetic resonance imaging-guided focused ultrasound ablation of uterine fibroids: early clinical experience. Radiat Med 2008; 26:198–205.
12. Funaki K, Fukunishi H, Sawada K. Clinical outcomes of magnetic resonance-guided focused ultrasound surgery for uterine myomas: 24-month follow-up. Ultrasound Obstet Gynecol 2009; 34:584–589.
13. LeBlang SD, Hoctor K, Steinberg FL. Leiomyoma shrinkage after MRI-guided focused ultrasound treatment: report of 80 patients. AJR Am J Roentgenol 2010; 194:274–280.
14. Kim YS, Keserci B, Partanen A, et al. Volumetric MR-HIFU ablation of uterine fibroids: role of treatment cell size in the improvement of energy efficiency. Eur J Radiol 2012; 81:3652–3659.
15. Ikink ME, Voogt MJ, Verkooijen HM, et al. Mid-term clinical efficacy of a volumetric magnetic resonance-guided high-intensity focused ultrasound technique for treatment of symptomatic uterine fibroids. Eur Radiol 2013; 23:3054–3061.
16. Park MJ, Kim YS, Rhim HC, et al. Safety and therapeutic efficacy of complete or near- complete ablation of symptomatic uterine fibroid tumors by MR imaging-guided high-intensity focused US therapy. J Vasc Interv Radiol 2014; 25:231–239.
17. Mindjuk I, Trumm CG, Herzog P, et al. MRI predictors of clinical success in MR-guided focused ultrasound (MRgFUS) treatments of uterine fibroids: results from a single centre. Eur Radiol 2015; 25:1317–1328.
18. Thiburce AC, Frulio N, Hocquelet A, et al. Magnetic resonance-guided high-intensity focused ultrasound for uterine fibroids: mid-term outcomes of 36 patients treated with the Sonalleve system. Int J Hyperthermia 2015; 31:764–770.
19. Kim YS, Kim BG, Rhim H, et al. Uterine fibroids: semiquantitative perfusion MR imaging parameters associated with the intra-procedural and immediate postprocedural treatment efficiencies of MR imaging-guided high-intensity focused ultrasound ablation. Radiology 2014; 273:462–471.
20. Kim YS, Lim HK, Park MJ, et al. Screening magnetic resonance imaging-based prediction model for assessing immediate therapeutic response to magnetic resonance imaging-guided high-intensity focused ultrasound ablation of uterine fibroids. Invest Radiol 2016; 51:15–24.
21. Kim YS, Lee JW, Choi CH, et al. Uterine fibroids: correlation of T2 signal intensity with semiquantitative perfusion MR parameters in patients screened for MR-guided high-intensity focused ultrasound ablation. Radiology 2016; 278:925–935.
22. Keserci B, Nguyen MD. Magnetic resonance-guided high-intensity focused ultrasound ablation of uterine fibroids: T1 perfusion based time-signal intensity curves in screening MRI as predictor of immediate non-perfused volume and treatment outcome. Eur Radiol 2017; 27:5299–5308.
23. Köhler MO, Mougenot C, Quesson B, et al. Volumetric HIFU ablation under 3D guidance of rapid MRI thermometry. Med Phys 2009; 36:3521–3535.

24. Spies JB, Coyne K, Guaou N, et al. The UFS-QOL, a new disease-specific symptom and health-related quality of life questionnaire for leiomyomata. Obstet Gynecol 2002; 99:290–300.
25. Sacks D, McClenny TE, Cardella J, et al. Society of Interventional Radiology clinical practice guidelines. J Vasc Interv Radiol 2003; 14:199–202.
26. Practice Committee of the American Society for Reproductive Medicine. Testing and interpreting measures of ovarian reserve: a committee opinion. Fertil Steril 2015; 103:9–17.
27. Henriques FC, Moritz AR. Studies of thermal injury in the conduction of heat to and through skin and the temperatures attained therein: a theoretical and experimental investigation. Am J Pathol 1947; 23:531–549.
28. Anderson GS. Human morphology and temperature regulation. Int J Biometeorol 1999; 43:99–109.
29. Cohen ML. Measurement of the thermal properties of human skin: a review. J Invest Dermatol 1977; 69:333–338.
30. Heinonen I, Kemppainen J, Kaskinoro K, et al. Capacity and hypoxic response of subcutaneous adipose tissue blood flow in humans. Circ J 2014; 78:1501–1506.
31. Yamashita Y, Torashima M, Takahashi M, et al. Hyperintense uterine leiomyoma at T2-weighted MR imaging: differentiation with dynamic enhanced MR imaging and clinical implications. Radiology 1993; 189:721–725.
32. Zhao WP, Chen JY, Zhang L, et al. Feasibility of ultrasound-guided high intensity focused ultrasound ablating uterine fibroids with hyperintense on T2-weighted MR imaging. Eur J Radiol 2013; 82:43–49.
33. Yoon SW, Lee C, Kim KA, et al. Contrast-enhanced dynamic MR imaging of uterine fibroids as a potential predictor of patient eligibility for MR guided focused ultrasound (MRgFUS) treatment for symptomatic uterine fibroids. Obstet Gynecol Int 2010; 2010:1–4. Article ID:834275.
34. Pennes HH. Analysis of tissue and arterial blood temperatures in the resting human forearm. J Appl Physiol 1948; 1:93–122.
35. Zhao WP, Chen JY, Chen WZ. Effect of biological characteristics of different types of uterine fibroids, as assessed with T2-weighted magnetic resonance imaging, on ultrasound-guided high intensity focused ultrasound ablation. Ultrasound Med Biol 2015; 41:423–431.
36. Arthur R, Kachura J, Liu G, et al. Laparoscopic myomectomy versus uterine artery embolization: long-term impact on markers of ovarian reserve. J Obstet Gynaecol Can 2014; 36:240–247.
37. Hehenkamp WJ, Volkers NA, Broekmans FJ, et al. Loss of ovarian reserve after uterine artery embolization: a randomized comparison with hysterectomy. Hum Reprod 2007; 22:1996–2005.
38. Kim CH, Shim SH, Jang H, et al. The effects of uterine artery embolization on ovarian reserve. Eur J Obstet Gynecol Reprod Biol 2016; 206:172–176.
39. Cheung VY, Lam TP, Jenkins CR, et al. Ovarian reserve after ultrasound-guided high-intensity focused ultrasound for uterine fibroids: preliminary experience. J Obstet Gynaecol Can 2016; 38:357–361.
40. Lee JS, Hong GY, Lee KH, et al. Changes in anti-Müllerian hormone levels as a biomarker for ovarian reserve after ultrasound-guided high-intensity focused ultrasound treatment of adenomyosis and uterine fibroid. BJOG 2017; 124:18–22.